Comparison of the Morphological and Biomechanical Characteristics of Keratoconus, Forme Fruste Keratoconus, and Normal Corneas

Li-Li Guo
Beijing Tongren Hospital, Capital Medical University
Lei Tian (tianlei0131@163.com)
Beijing Tongren Hospital, Capital Medical University
Kai Cao
Beijing Tongren Hospital, Capital Medical University
Yu-Xin Li
Beijing Tongren Hospital, Capital Medical University
Na Li
Beijing Tongren Hospital, Capital Medical University
Wei-Qiang Yang
Beijing Tongren Hospital, Capital Medical University
Ying Jie
Beijing Tongren Hospital, Capital Medical University

Research Article

Keywords: keratoconus, forme fruste keratoconus, corneal morphology, corneal biomechanics

Posted Date: December 15th, 2020

DOI: https://doi.org/10.21203/rs.3.rs-124253/v1

Abstract

Background: To explore the feasibility of corneal morphological and biomechanical parameters for keratoconus and forme fruste keratoconus diagnosis.

Methods: This case-control study included a total of 517 eyes from 408 keratoconus patients (KC group), 83 eyes from 83 forme fruste keratoconus patients (FFKC group), and 158 eyes from 158 patients with normal corneas (NL group). All subjects underwent routine ophthalmology examinations. Pentacam and Corneal Visualization Scheimpflug Technology were used to obtain corneal morphological and biomechanical parameters. Differences between the groups were compared using receiver operating characteristic (ROC) curve analysis.

Results: Comparison of the NL group with the KC and FFKC groups (P<0.05), and the NL and KC groups alone (P<0.017), revealed statistically significant differences in corneal morphological and biomechanical parameters, except time from the start until the highest concavity (HCT), deflection length of the first applanation (A1 DfL), and deflection length of the second applanation (A2 DfL). Comparison of the NL and FFKC groups revealed 12 significantly different parameters (P<0.017). ROC analysis showed that all corneal morphological parameters and most biomechanical parameters distinguished KC from NL, with an area under the curve (AUC) greater than 0.80, of which Belin-Ambrósio enhanced ectasia total deviation index (BAD-D) and tomographic and biomechanical index (TBI) were most efficient. Except for central astigmatism from the anterior corneal surface (AstigF), the AUC that distinguished FFKC from NL was 0.862. Other parameters distinguished FFKC from NL with low efficiency.

Conclusion: All corneal morphological and most biomechanical parameters are different in KC versus NL, but only a few parameters are different in FFKC versus NL. BAD-D and TBI have the highest efficiency, sensitivity, and specificity for distinguishing KC from NL. The parameters had a low ability to distinguish FFKC from NL. The application of biomechanical instruments to diagnose early keratoconus needs further study.

1. Introduction

Keratoconus is the most common corneal ectasia disease, mainly manifested as non-inflammatory, progressive thinning and bulging in the central or paracentral cornea, causing high astigmatism and corneal scarring [1]. Patients with keratoconus are mostly adolescents, 90% of whom develop keratoconus in both eyes, and the course of the disease is often asymmetric [2, 3]. During the progression of the disease, the elastic layer of the cornea fractures, and the composition of collagen fibers and the material between collagen fibers become disordered and unbalanced. Protein kinases and other catabolic enzymes in the cornea increase and levels of protein kinase inhibitors decrease, causing the corneal cross-linking structure to deteriorate and the corneal stroma to decrease and resulting in unstable corneal biomechanical properties and weakened mechanical strength [4, 5]. Therefore, the diagnosis of keratoconus using the biomechanical properties of the cornea has become a hot topic in recent research.

In vivo corneal biomechanical measurement equipment used only in the clinic include the Ocular Response Analyzer (ORA) [6] and the Corneal Visualization Scheimpflug Technology (Corvis ST) [7]. Both devices use the corneal response to rapid air pulses to indirectly assess the biomechanical properties of the cornea [8]. The parameters provided by the ORA to reflect the biomechanical properties of the cornea are corneal hysteresis (CH) and the corneal resistance factor (CRF). Although studies have reported that CH and CRF in keratoconus are lower than those in healthy corneas, the distribution of these two parameters has more overlap, and the sensitivity and

specificity for diagnosing keratoconus are relatively weak [9]. Studies have shown that the biomechanical parameters measured in the early version of Corvis ST (1.00r30) proved to be significantly different between keratoconus patients and healthy people, and that the deformation amplitude (DA) has better diagnostic efficiency for keratoconus. However, this parameter is susceptible to the influence of intraocular pressure (IOP), and its efficiency in early keratoconus diagnosis is not high [10]. With the update to the Corivs ST software (software version 1.5r1902), some new parameters appeard, such as the maximal value of the ratio between the deformation amplitude at the apex and at 2 mm from the corneal apex (DA Ratio 2), Ambrósio relational thickness to the horizontal profile (ARTh), Inverse of the radius of curvature during the concave phase of the deformation (Integrated Radius), stiffness parameter at the first applanation (SPA1), Corvis biomechanical index (CBI) and tomographic and biomechanical index (TBI) etc. Additionally, there are studies shown that some new parameters have higher efficiency in the diagnosis of keratoconus [11, 12]. However, little research has been conducted on the diagnostic efficiency of Corvis ST biomechanical parameters for keratoconus and forme fruste keratoconus, and the research results are not consistent [7, 12–14].

In this study, Pentacam and Corvis ST measurements were used to compare the corneal morphological and biomechanical characteristics of keratoconus, forme fruste keratoconus, and normal corneas in patients in China. Our research aimed to investigate the relationship between corneal morphological and biomechanical parameters and keratoconus, as well as to explore the diagnostic efficiency of these parameters especially the new parameters for early keratoconus.

2. Materials And Methods

2.1 Research subjects

A total of 517 eyes from 408 patients with keratoconus (KC group), 83 eyes from 83 patients with forme fruste keratoconus (FFKC group), and 158 eyes from 158 normal volunteers (NL group) were included in this study. Patients with keratoconus diagnosed in both eyes had both included in the study. The right eye was selected for study in the NL group. This study complied with the Declaration of Helsinki and was approved by the Ethics Committee of Beijing Tongren Hospital. All selected candidates signed informed consent forms.

2.2 Inclusion criteria

2.2.1 Inclusion criteria for the KC group

The Rabinowitz standard was used for the diagnosis of keratoconus [15]. The inclusion criteria for the KC group were as follows: (1) Patients had a history of myopia and astigmatism; decreased vision; corrected visual acuity was less than 1.0; at least one of the following signs during slit-lamp examination: corneal stroma thinning, conical forward ectasia, Fleischer ring, Vogt line, epithelium or epithelium Subcutaneous scars; corneal topographic examination showed that the diopter of the central area of the anterior corneal surface was more than 47 D; the difference between the diopter of the lower and upper 3 mm of the central corneal area was more than 3 D; the difference between the corneal diopter in both eyes of the same patient was more than 1 D. (2) The diopter at the center of the cornea was more than 46.5 D; the difference between the corneal diopter of the lower and upper 3 mm of the cornea was more than 1.26 D; the difference between the corneal diopter in both eyes of the same patient was more than 0.92 D.

2.2.2 Inclusion criteria for the FFKC group

The diagnostic criteria for the FFKC group were as follows [16]: One eye of the patient was diagnosed with keratoconus, and there was no corneal topography abnormality in the contralateral eye; standards of the normal corneal topography [12] [17] were that the posterior corneal height at the thinnest cornea was less than 15 μm, the Ambrosio-related maximum thickness was greater than 339, and the Belin-Ambrósio enhanced ectasia total deviation index (BAD-D) was less than 1.6.

2.2.3 Inclusion critera for the NL group

After the KC group and the FFKC group were enrolled, patients with stable vision and normal corneal topography before refractive surgery were included (excluding other eye diseases, except for myopia).

2.3 Exclusion criteria

All study enrollees excluded patients with eye diseases other than keratoconus, trauma, and surgical history. Patients with systemic diseases that can affect the eyes were also excluded from the study. Soft contact lens wearers were required to stop wearing contact lenses for more than two weeks. Hard contact lens wearers were required to stop wearing contact lenses for more than one month.

2.4 Inspection items

All enrolled subjects underwent routine ophthalmology examinations, including uncorrected distant vision, slit lamp microscope examination, and fundus examination. At the same time, Pentacam was used to obtain corneal morphological parameters, and Corvis ST was used to obtain corneal biomechanical parameters.

Pentacam (Oculus, Germany, software version 1.20r134) is a currently commonly used corneal tomography analysis instrument. This instrument scans the anterior surface of the cornea to the posterior surface of the crystalline lens through the Scheimpflug camera, and calculates and analyzes the collected data through the software to obtain the morphological parameters of the anterior segment.

Corvis ST (Oculus, Germany, software version 1.5r1902) adopts air-pressing technology to cause corneal indentation deformation and uses a Scheimpflug high-speed camera to record the entire process. This instrument particularly monitors and analyzes the deformation process of the bidirectional applanation and the highest concavity state. Thus, it is possible to obtain parameters that reflect the corneal biomechanical characteristics.

The same skilled technician operated the Pentacam and Corvis ST instruments between 8:00–17:00. The best quality pictures were used for observation. The displayed “OK” message indicated that the measurement quality was good, and the corresponding data was recorded. Table 1 shows the Pentacam and Corvis ST parameters included in this study.

Table 1
Corneal tomographic and deformation parameters provided by the Pentacam and Corvis Scheimpflug Technology instruments.

Parameters	Parameters
Pentacam	A2V the second velocity of applanation
K1 steepest keratometric reading	
K2 flattest keratometric reading	HCT time from the start until the highest concavity
Km F mean keratometry from the anterior corneal surface	PD peak distance
Kmax maximum keratometry from the anterior corneal surface	Radius central curvature radius at the highest concavity
AstigF central astigmatism from the anterior corneal surface	A1 DfL deflection length of the first applanation
CCT corneal thickness at the apex of the cornea	HC DfL deflection length of the highest concavity
TP pachymetry at the thinnest point	A2 DfL deflection length of the second applanation
ISV index of surface variance	A1 DfA deflection amplitude of the first applanation
IVA index of vertical asymmetry	HC DfA deflection amplitude of the highest concavity
KI keratoconus index	A2 DfA deflection amplitude of the second applanation
CKI central keratoconus index	DA Ratio2 the maximal value of the ratio between the deformation amplitude at the apex and at 2 mm from the corneal apex
IHA index of height asymmetry	DA Ratio1 the maximal value of the ratio between the deformation amplitude at the apex and at 1 mm from the corneal apex
IHD index of height decentration	ARTh Ambrósio relational thickness to the horizontal profile
BAD-D Belin-Ambrósio enhanced ectasia total deviation index	bIOP biomechanical-corrected intraocular pressure
A1T first applanation time	Integrated Radius inverse of the radius of curvature during the concave phase of the deformation
Corvis ST	
A1V first velocity of applanation	SPA1 stiffness parameter at the first applanation
A2T second applanation time	CBI Corvis biomechanical index
	TBI tomographic and biomechanical index

2.5 Statistical methods

R language 4.0 was used for statistical analysis and drawing of the results. The Shapiro-Wilk test was used to test the normality of the corneal morphological and biomechanical parameters. The mean ± standard deviation was used for the basic statistical description of the measured data that followed a normal distribution. The median and quartile range were used for basic statistical description of non-normal data. The Kruskal-Wallis test was used to compare the parameters of the KC group, FFKC group, and NL group. A $P < 0.05$ was considered

statistically significant. A post-hoc test was used for comparison between two groups. Since multiple comparisons were involved when comparing the KC group, FFKC group, and NL group in pairs, the comparison level was adjusted to 0.017 according to the Bonferroni principle. Thus, a $P < 0.017$ was considered significantly different. Receiver operating characteristic (ROC) curve analysis was used to explore the ability of each corneal morphological parameter and biomechanical parameter to distinguish between keratoconus, forme fruste keratoconus, and normal corneas. The DeLong test was used to compare differences between the area under the curve (AUC) of the different parameters. Since the ROC curve was involved in multiple comparisons when comparing groups in pairs, the inspection level was corrected to 0.0023 according to the Bonferroni principle.

3. Results

3.1 Study participant characteristics

There were a total of 758 eyes from 581 patients included in this study. The KC group included 517 eyes from 408 cases, of which 289 cases were male and 228 cases were female, and the average age was 22.56 ± 7.77 years old (range: 13–45 years old). The FFKC group included 83 eyes from 83 cases, of which 49 cases were male and 34 cases were female, and the average age was 22.38 ± 9.23 years old (range: 16–45 years old). The NL group included 158 eyes from 158 cases, of which 99 cases were male and 59 were female, and the average age was 23.08 ± 4.6 years old (range: 18–36 years old). There was no statistically significant difference between the age groups of the KC, FFKC, and NL groups ($P = 0.085$). Furthermore, there was no statistically significant difference between gender distribution in the three groups ($P = 0.311$), where chi-square tests showed (NL vs KC: $P = 0.133$, NL vs FFKC: $P = 0.583$, and KC vs FFKC: $P = 0.593$) for gender distribution in the KC, FFKC, and NL groups, respectively.

3.2 Comparison between groups

Among the corneal morphological and biomechanical parameters, except for HCT, A1 DfL, A2 DfL, all other parameters revealed significant differences among the three groups. Significant differences are indicated as $P < 0.05$. The data are shown in Table 2.

Table 2
Results from comparisons of each parameter between the keratoconus (KC) group, forme fruste keratoconus (FFKC) group, and normal cornea (NL) group (median and range of variation)

Parameters	NL group	KC group	FFKC group	*P* (NL, KC, FFKC)	*P* (NL vs KC)	*P* (NL vs FFKC)	*P* (KC vs FFKC)
K1	42.40 (41.50–43.30)	45.60 (43.30–49.30)	42.40 (41.50–43.60)	< 0.001	< 0.001	0.812	< 0.001
K2	43.95 (43.00–44.90)	48.90 (46.30–53.80)	43.70 (42.80–45.00)	< 0.001	< 0.001	0.586	< 0.001
Km	43.20 (42.40–44.00)	47.20 (44.60–51.30)	43.10 (42.10–44.20)	< 0.001	< 0.001	0.828	< 0.001
Kmax	44.40 (43.70–45.60)	54.00 (49.10–62.30)	44.50 (43.50–45.60)	< 0.001	< 0.001	0.907	< 0.001
AstigF	1.20 (0.80–1.90)	3.30 (2.00–4.80)	22.40 (2.60–169.10)	< 0.001	< 0.001	< 0.001	< 0.001
CCT	553.59 (537.63–578.00)	472.00 (439.00–504.00)	527.00 (513.65–552.00)	< 0.001	< 0.001	< 0.001	< 0.001
TP	548.00 (533.00–573.00)	461.00 (429.00–493.00)	525.00 (508.00–545.00)	< 0.001	< 0.001	< 0.001	< 0.001
ISV	17.00 (14.00–22.00)	75.00 (46.00–112.00)	18.00 (15.00–23.00)	< 0.001	< 0.001	0.238	< 0.001
IVA	0.11 (0.08–0.15)	0.68 (0.39–1.02)	0.13 (0.10–0.17)	< 0.001	< 0.001	0.001	< 0.001
KI	1.03 (1.01–1.04)	1.17 (1.10–1.28)	1.03 (1.02–1.05)	< 0.001	< 0.001	0.075	< 0.001
CKI	1.01 (1.00–1.01)	1.05 (1.02–1.12)	1.01 (1.00–1.01)	< 0.001	< 0.001	0.223	< 0.001
IHA	5.40 (2.10–9.70)	22.20 (12.50–38.90)	4.90 (1.90–8.70)	< 0.001	< 0.001	0.998	< 0.001
IHD	0.01 (0.01–0.01)	0.10 (0.05–0.16)	0.01 (0.01–0.02)	< 0.001	< 0.001	0.008	< 0.001
BAD	0.96 (0.53–1.29)	7.58 (4.49–11.79)	1.28 (0.75–1.62)	< 0.001	< 0.001	< 0.001	< 0.001
A1T	7.40 (7.24–7.59)	7.02 (6.87–7.21)	7.27 (7.08–7.44)	< 0.001	< 0.001	< 0.001	< 0.001
A1V	0.15 (0.13–0.16)	0.17 (0.16–0.19)	0.16 (0.14–0.17)	< 0.001	< 0.001	0.002	< 0.001

Parameters	NL group	KC group	FFKC group	*P* (NL, KC, FFKC)	*P* (NL vs KC)	*P* (NL vs FFKC)	*P* (KC vs FFKC)
A2T	21.81 (21.52–22.04)	22.12 (21.83–22.35)	21.99 (21.68–22.22)	< 0.001	< 0.001	0.019	0.004
A2V	-0.27 (-0.29–-0.25)	-0.32 (-0.36–-0.28)	-0.28 (-0.31–-0.25)	< 0.001	< 0.001	0.042	< 0.001
HCT	16.86 (16.63–17.13)	16.86 (16.63–17.09)	16.91 (16.63–17.32)	0.465	0.381	0.686	0.314
PD	5.17 (4.96–5.28)	5.21 (5.06–5.38)	5.18 (4.97–5.35)	0.007	0.002	0.324	0.204
Radius	7.31 (6.95–7.94)	5.55 (4.84–6.42)	6.88 (6.50–7.31)	< 0.001	< 0.001	< 0.001	< 0.001
A1 DfL	2.33 (2.22–2.42)	2.36 (2.24–2.48)	2.33 (2.26–2.43)	0.054	0.018	0.424	0.354
HC DfL	6.70 (6.34–6.96)	6.54 (6.18–6.83)	6.68 (6.31–7.06)	0.000	0.001	0.946	0.009
A2 DfL	2.80 (2.56–3.42)	2.86 (2.44–3.55)	2.89 (2.47–3.51)	0.990	0.955	0.866	0.910
A1 DfA	0.10 (0.09–0.10)	0.11 (0.10–0.12)	0.10 (0.09–0.10)	< 0.001	< 0.001	0.013	< 0.001
HC DfA	0.91 (0.85–0.97)	1.07 (0.97–1.18)	0.94 (0.87–1.02)	< 0.001	< 0.001	0.018	< 0.001
A2 DfA	0.11 (0.10–0.12)	0.12 (0.11–0.14)	0.11 (0.10–0.12)	< 0.001	< 0.001	0.009	0.001
DA Ratio 2	4.06 (3.85–4.30)	5.67 (4.79–6.52)	4.38 (4.06–4.78)	< 0.001	< 0.001	< 0.001	< 0.001
DA Ratio 1	1.54 (1.52–1.58)	1.67 (1.60–1.74)	1.57 (1.54–1.60)	< 0.001	< 0.001	0.001	< 0.001
ARTh	452.06 (390.36–524.38)	212.10 (139.63–303.59)	454.96 (398.38–516.43)	< 0.001	< 0.001	0.743	< 0.001
bIOP	14.90 (13.70–15.82)	14.05 (12.70–15.30)	14.50 (13.30–15.80)	< 0.001	< 0.001	0.286	0.026
Integrated Radius	7.75 (7.31–8.35)	11.31 (9.56–13.24)	8.51 (7.77–9.20)	< 0.001	< 0.001	< 0.001	< 0.001
SPA1	107.21 (96.17–117.78)	58.84 (43.91–75.02)	91.85 (80.87–101.90)	< 0.001	< 0.001	< 0.001	< 0.001
CBI	0.01 (0.00–0.07)	1.00 (0.96–1.00)	0.07 (0.01–0.40)	< 0.001	< 0.001	< 0.001	< 0.001

Parameters	NL group	KC group	FFKC group	*P* (NL, KC, FFKC)	*P* (NL vs KC)	*P* (NL vs FFKC)	*P* (KC vs FFKC)
TBI	0.14 (0.02–0.26)	1.00 (1.00–1.00)	0.29 (0.14–0.51)	< 0.001	< 0.001	< 0.001	< 0.001

The comparison results of the parameters between the NL group, the KC group, and the FFKC group were further paired: When the NL group and the KC group were compared, the differences in morphological parameters were found to be statistically significant ($P < 0.001$). Except for HCT, A1 DfL, and A2 DfL, all the other biomechanical parameters showed statistically significant differences, as well ($P < 0.017$). Comparing the NL group with the FFKC group, AstigF, TP, CCT, IVA,and BAD-D had statistically significant differences ($P < 0.017$). Among the biomechanical parameters, A1T, A1V, Radius, A1 DfA, A2 DfA, DA Ratio1, DA Ratio2, Integrated Radius, SPA1, CBI, and TBI were statistically significant ($P < 0.017$). The data are shown in Table 2.

3.3 ROC curve of each parameter

ROC curve analysis showed that the measured corneal morphological parameters of the NL group and the KC group had an AUC greater than 0.80. BAD-D had the largest AUC (0.989). Most biomechanical parameters were able to effectively distinguish keratoconus from a normal cornea. Radius, DA Ratio2, Integrated Radius, ARTh, SPA1, CBI, and TBI were all effective in diagnosing keratoconus, with an AUC greater than 0.90. Among all corneal morphological and biomechanical parameters measured, BAD-D and TBI were the most efficient in distinguishing between the NL and KC groups. The data are shown in Table 3.

Table 3
Receiver operator characteristic curve analysis results for the different parameters distinguishing the keratoconus (KC) group and forme fruste keratoconus (FFKC) group from the normal cornea (NL) group

	KC group vs NL group				FFKC group vs NL group			
	AUC (95% CI)	Cutoff	Sensitivity, %	Specificity,%	AUC (95% CI)	Cutoff	Sensitivity, %	Specificity,%
K1	0.814	43.75	0.696	0.873	0.509	43.45	0.289	0.784
K2	0.907	46.35	0.746	0.962	0.521	43.75	0.518	0.582
Km	0.873	44.45	0.783	0.867	0.508	42.55	0.398	0.696
Kmax	0.966	46.85	0.897	0.949	0.505	46.65	0.145	0.924
AstigF	0.827	2.35	0.685	0.861	0.862	4.65	0.735	0.993
CCT	0.944	517.34	0.83	0.956	0.714	527.5	0.506	0.861
TP	0.954	518.5	0.894	0.93	0.728	531.5	0.590	0.797
ISV	0.987	30.5	0.979	0.956	0.546	22.50	0.277	0.816
IVA	0.985	0.215	0.954	0.956	0.625	0.085	0.904	0.329
KI	0.985	1.055	0.981	0.943	0.569	1.045	0.313	0.854
CKI	0.887	1.015	0.799	0.962	0.458	1.025	0.012	1
IHA	0.864	13.05	0.731	0.924	0.499	8.05	0.722	0.335
IHD	0.981	0.025	0.917	0.981	0.603	0.013	0.445	0.747
BAD	0.989	1.595	0.959	1	0.684	1.465	0.422	0.930
A1T	0.855	7.13	0.652	0.911	0.660	7.33	0.674	0.601
A1V	0.819	0.161	0.7	0.791	0.623	0.157	0.469	0.734
A2T	0.691	21.912	0.687	0.658	0.592	21.96	0.542	0.696
A2V	0.766	-0.314	0.559	0.937	0.58	-0.302	0.313	0.867
HCT	0.477	17.02	0.412	0.608	0.516	16.907	0.518	0.576
PD	0.581	5.288	0.394	0.76	0.539	5.288	0.361	0.759
Radius	0.912	6.581	0.807	0.924	0.681	6.946	0.566	0.753
A1 DfL	0.562	2.435	0.313	0.816	0.469	2.361	0.626	0.398
HC DfL	0.59	6.497	0.479	0.709	0.497	6.511	0.373	0.696
A2 DfL	0.502	4.005	0.135	0.949	0.493	4.353	0.084	0.993
A1 DfA	0.765	0.103	0.563	0.879	0.597	0.095	0.663	0.494

AUC: area under the receiver operating characteristic curve.

	KC group vs NL group				FFKC group vs NL group			
HC DfA	0.824	0.973	0.747	0.778	0.593	0.972	0.398	0.778
A2 DfA	0.706	0.113	0.619	0.728	0.603	0.108	0.602	0.563
DA Ratio 2	0.921	4.742	0.768	0.975	0.712	4.464	0.482	0.886
DA Ratio 1	0.887	1.604	0.749	0.918	0.629	1.561	0.614	0.652
ARTh	0.9	328.6	0.783	0.981	0.487	395.744	0.783	0.272
bIOP	0.624	14.696	0.64	0.576	0.542	14.55	0.530	0.589
Integrated Radius	0.93	9.024	0.82	0.949	0.705	8.412	0.566	0.791
SPA1	0.94	79.13	0.802	0.981	0.761	96.71	0.699	0.741
CBI	0.916	0.516	0.845	1	0.667	0.067	0.518	0.749
TBI	0.993	0.515	0.967	1	0.722	0.273	0.554	0.797

AUC: area under the receiver operating characteristic curve.

ROC curve analysis of the NL and FFKC groups showed an AUC less than 0.87 when measuring corneal morphological parameters. The morphological parameters with relatively high AUCs were BAD-D, AstigF, CCT, and TP (AUC range: 0.684–0.862). When using biomechanical parameters, the efficiency of distinguishing between the FFKC and NL groups was low, and the parameters with relatively high diagnostic efficiencies were Radius, DA Ratio2, Integrated Radius, SPA1, CBI, and TBI (AUC range: 0.667–0.761). The data are shown in Table 3.

Comparing the diagnostic capabilities of various parameters for keratoconus and forme fruste keratoconus using ROC curves of BAD-D, DA Ratio2, ARTh, Integrated Radius, SPA1, CBI, and TBI, we found that these parameters could effectively diagnose keratoconus (AUC > 0.90). Figure 1 show the ROC. However, the efficiency of these parameters for diagnosing forme fruste keratoconus was low. Figure 2 show the ROC. The AUCs of BAD-D and TBI were statistically different from the AUCs of DA Ratio2, Integrated Radius, SPA1, and CBI. The AUC associated with BAD-D and TBI was greater than the AUC of the other parameters. Thus, the efficiency of BAD-D and TBI in diagnosing keratoconus was higher than the other parameters. However, the AUC of BAD-D and TBI were not statistically significant ($P = 0.232$); therefore, BAD-D and TBI had the highest efficiency in diagnosing keratoconus. The data are shown in Table 4. Furthermore, ARTh was statistically different than the other six parameters in the diagnosis of keratoconus and forme fruste keratoconus ($P < 0.0023$), and ARTh had the lowest ability in diagnosing forme fruste keratoconus. However, there was no statistically significant difference between the AUC of ARTh and the other parameters. The data are shown in Table 4

Table 4
Comparison of the receiver operator characteristic curves

The parametric curves compared		*P* (KC vs NL)	*P* (FFKC vs NL)
BAD-D	DA Ratio2	< 0.001	0.572
	ARTh	< 0.001	0.001
	Integrated Radius	< 0.001	0.669
	SPA1	< 0.001	0.099
	CBI	< 0.001	0.703
	TBI	0.232	0.285
DA Ratio2	ARTh	0.044	< 0.001
	Integrated Radius	0.228	0.833
	SPA1	0.024	0.165
	CBI	0.597	0.237
	TBI	< 0.001	0.833
ARTh	Integrated Radius	0.009	< 0.001
	SPA1	0.021	< 0.001
	CBI	0.017	0.014
	TBI	< 0.001	< 0.001
Integrated Radius	SPA1	0.266	0.116
	CBI	0.180	0.395
	TBI	< 0.001	0.714
SPA1	CBI	0.003	0.016
	TBI	< 0.001	0.348
CBI	TBI	< 0.001	0.252

4. Discussion

Keratoconus is a localized corneal ectasia disease that can cause a serious drop in corneal optical performance and a slow decline in visual asymmetry. Keratoconus is an absolute contraindication to corneal refractive surgery; thus, accurate preoperative diagnosis is particularly important. Although the diagnosis of keratoconus in clinical maturity and progression is not difficult, the diagnosis of keratoconus in the subclinical stage is still challenging [18]. At present, the auxiliary methods for diagnosing keratoconus are mainly corneal topography and corneal tomography, but these two methods are susceptible to tear film, ocular surface diseases, and contact lens wear. The diagnosis of subclinical keratoconus has some limitations [19]. Subclinical keratoconus has long been regarded as one of the most important independent risk factors for the occurrence of iatrogenic keratopathy.

Studies have shown that changes in corneal biomechanics may occur before changes in typical corneal morphology [20]. In recent years, the biomechanical research of early keratoconus has become a hot topic. In this study, we comparatively analyzed the corneal morphological and biomechanical characteristics of keratoconus, forme fruste keratoconus, and normal corneas, and further analyzed the diagnostic efficiency of various morphological and biomechanical parameters for keratoconus and forme fruste keratoconus.

Wahba et al. [21] found that corneal morphological parameters have significant statistical differences between normal corneas and keratoconus. In this study, there was a statistically significant difference in all corneal morphological parameters between the normal cornea and keratoconus groups. The corneal curvature, astigmatism, and corneal index of the keratoconus group were significantly higher than those of the normal cornea group, while corneal thickness was significantly smaller than that of the normal cornea group.

Many studies have found that the corneal morphological parameters have a higher ability to distinguish keratoconus from normal corneas, and the BAD-D parameter has higher efficiency, sensitivity, and specificity in distinguishing between normal corneas and keratoconus [22–24]. In a study of 21 cases of keratoconus and 78 cases of the normal cornea, Wang YM et al. [24] found that BAD-D distinguishes between normal and keratoconus with an AUC of 1.00, cut-off point of 1.54, sensitivity of 1.00, and specificity of 0.803. In this study, all corneal morphological parameters had higher efficiency in distinguishing between normal corneas and keratoconus, with an AUC greater than 0.81. Furthermore, BAD-D had the highest diagnostic efficiency for distinguishing between keratoconus and normal corneas with an AUC of 0.989, cut-off point of 1.595, as well as a sensitivity and specificity of 0.959 and 1.00, respectively.

Scarcelli et al. [25] suggested that keratoconus is initially caused by the local weakening of corneal biomechanical properties. Over time, under the same IOP, the mechanical strength of the cornea weakens, the mechanical strength of the local area of soft tissue becomes stronger than the surrounding area, and the ability to resist IOP worsens, resulting in an increase in the curvature and thinning of the softer corneal area. Based on these findings, keratoconus may be identified during the biomechanical change stage, before the cornea becomes thinner and more curved.

Earlier studies on keratoconus biomechanics found that the differences in biomechanical parameters between the the normal cornea group and keratoconus group were statistically significant, and the AUC of the parameters overlapped between 0.673 and 0.852 [10, 26, 27]. With the introduction of new Corvis ST parameters, more related studies have appeared. Research by Vinciguerra et al. [28] found that CBI has the highest efficiency in distinguishing keratoconus and normal cornea in biomechanical parameters, with a sensitivity and specificity of 1.00 and 0.984, respectively. Our previous study found that [10], among the biomechanical parameters, DA had the highest efficiency in diagnosing keratoconus, with an AUC of 0.882. However, this parameter has significant overlap in the keratoconus group and the control group. In this study, when comparing the normal group with the keratoconus group, most of the biomechanical parameters were significantly different, and most biomechanical parameters could effectively diagnose keratoconus. The parameters proposed by the new version of the software, such as DA Ratio2, Integrated Radius, ARTh, SPA1, and CBI, had higher diagnostic efficiency for keratoconus, with an AUC greater than 0.90, among which SPA1 had the largest AUC (0.94), and a sensitivity and specificity of 0.802 and 0.981, respectively. Although CBI had an AUC value of 0.916 (the cut-off point: 0.516) for distinguishing between keratoconus and normal cornea, its sensitivity and specificity were the highest (0.845 and 1.00, respectively). This is similar to previous research results [28].

In the past two years, Ambrosio et al. [11] have developed a new parameter, TBI, and applied it to the keratoconus study. They found that TBI was more efficient than previously analyzed parameters in detecting corneal ectasia diseases, with an AUC of 1.00. When the TBI value was 0.79, the sensitivity and specificity values were both equal to 1.00. In this study, the AUC for TBI to distinguish between keratoconus and normal corneas was 0.993; and, when the value was 0.515, the sensitivity and specificity values were 0.967 and 1.00, respectively. The difference between the AUCs of TBI and BAD-D was not statistically significant; therefore, these two parameters are the most efficient in diagnosing keratoconus.

Keratoconus is typically a binocular disease. When a patient suffers the onset of keratoconus in one eye, the other eye may develop the same disease within a few years [17, 29]. Forme fruste keratoconus in a relatively healthy eye may represent an earlier stage of the disease, and is currently undetectable by topography and tomography [19]. With the development of biomechanical instruments and the development of new parameters, many researchers have analyzed eyes affected by forme fruste keratoconus. Ambrosio et al. [11] reported that BAD-D, CBI, and TBI can effectively distinguish normal eyes from forme fruste keratoconus, and TBI has the highest diagnostic efficiency, with an AUC of 0.985, sensitivity of 0.904, and specificity of 0.96. Studies by Mingyue et al. [13] found that BAD-D, CBI, and TBI can effectively distinguish normal eyes from forme fruste keratoconus, and the diagnostic efficiency of CBI is the highest, with an AUC of 0.909, sensitivity of 0.903, and specificity of 0.917. In this study, the ability of BAD-D, CBI, and TBI to distinguish between normal corneas and forme fruste keratoconus was low, with an AUC of 0.684, 0.667, and 0.722, respectively. This is different from some previous reports [11, 13, 30], but similar to the report by Peng Song et al. [14]. Our analysis shows that the parameters in this study have a low ability to diagnose forme fruste keratoconus, mainly because the inclusion criteria for forme fruste keratoconus are different and this study excludes eyes with a BAD-D value greater than 1.6, unlike the study of Mingyue et al. [13]. In their study, the average BAD-D value of the forme fruste keratoconus group was 2.409. This is also different from the study by Pratik Kataria et al. [12], where the BAD-D value of the forme fruste keratoconus group ranged from − 0.82–3.35. Additionally, in this study, there may be some forme fruste keratoconus patients with normal eyes. These eyes may not have been diseased, or there may have been some true monocular keratoconus. Although studies have shown that true unilateral keratoconus does not exist [31]. However, Imbornoni et al. [32] reported five cases that may be true unilateral keratoconus, and the healthy eyes of these patients remained normal during 3 to 7 years of follow-up. Therefore, whether there is also true monocular keratoconus needs to be further investigated.

This study has a relatively large sample size and a large number of corneal morphological and biomechanical parameters are included, including some new parameters. Furthermore, this study also analyzed patients with forme fruste keratoconus, which may represent an earlier stage of the disease. The limitation of the study is that this is a cross-sectional study, and there is a lack of follow-up for patients with forme fruste keratoconus. Furthermore, there are relatively few cases of forme fruste keratoconus. In future studies, the sample size will be further increased and we will continue to follow-up the disease progression of patients with forme fruste keratoconus.

5. Conclusions

In summary, all corneal morphological parameters and most biomechanical parameters are highly effective in diagnosing keratoconus, of which BAD-D and TBI are the most efficient. The ability of all parameters to

distinguish normal corneas from forme fruste keratoconus was low (inclusion criteria: BAD-D<1.6). The application of biomechanical instruments to detect early keratoconus still requires further investigation.

Declarations

Ethics approval and consent to participate

This study complied with the Declaration of Helsinki and was approved by the Ethics Committee of Beijing Tongren Hospital. All selected candidates signed informed consent forms. For those minor candidates who are below 18 years, the informed consent was signed by their parents or their legal guardians.

Consent for publication

Not applicable.

Availability of data and materials

The datasets used and/or analysed during the current study are available from the corresponding author on reasonable request.

Competing interests

The authors declare that they have no competing interests.

Author contributions

Li-li Guo and Lei Tian contributed equally to this work.

LT: Corresponding author; conception and design of the study; LLG: acquisition of the data, drafting the article; LLG, KC: analysis and interpretation of the data; LLG, KC: analysis of the data; YXL, WQY: acquisition of the data. LT, NL, YJ: revise the article. All authors read and approved the final manuscript.

Funding

This research was supported by Grants from the National Natural Science Foundation of China (31600758); Beijing Nova Program (Z181100006218099); the Open Research Fund from Beijing Advanced Innovation Center for Big Data-Based Precision Medicine, Beijing Tongren Hospital, Beihang University & Capital Medical University (BHTR-KFJJ-202001).

Acknowledgements

Not applicable.

References

1. Rabinowitz Y S. Keratoconus. Survey of Ophthalmology. 1997;42(4): 297–319.
2. McMahon TT, Szczotka-Flynn L, Barr JT, Anderson RJ, Slaughter ME, Lass JH, et al. A New Method for Grading the Severity of Keratoconus: The Keratoconus Severity Score (KSS). Cornea. 2006;25(7):794–800.
3. Shirayama-Suzuki M, Amano S, Honda N, Usui T, Yamagami S, Oshika T. Longitudinal analysis of corneal topography in suspected keratoconus. Br J Ophthalmology. 2009;93(6): 815–819.
4. Meek KM, Tuft SJ, Huang Y, Gill PS, Hayes S, Newton RH, et al. Changes in collagen orientation and distribution in keratoconus corneas. Invest Ophthalmol Vis Sci. 2005;46: 1948–56.
5. Gefen A, Shalom R, Elad D, Mandel Y. Biomechanical analysis of the keratoconic cornea. J Mech Behav Biomed Mater. 2009;2(3):224–36.
6. Luce DA. Determining in vivo biomechanical properties of the cornea with an ocular response analyzer. J cataract refract surg. 2005;31(1): 156–162.
7. Hon Y, Lam AK. Corneal deformation measurement using Scheimpflug noncontact tonometry. Optom Vis Sci. 2013;90(1): e1-8.
8. Pi?Ero DP, Alcón, Natividad. In?vivo characterization of corneal biomechanics. J cataract refract surg. 2014;40(6):870–887.
9. Terai N, Raiskup F, Haustein M, Pillunat LE, Spoerl E. Identification of biomechanical properties of the cornea: the ocular response analyzer. Curr Eye Res. 2012;37(7): 553–562.
10. Tian L, Huang YF, Wang LQ, Bai H, Wang Q, Jiang JJ, et al. Corneal Biomechanical Assessment Using Corneal Visualization Scheimpflug Technology in Keratoconic and Normal Eyes. Journal Ophthalmol. 2014;2014:1–8.
11. Ambrósio R Jr, Lopes BT, Faria-Correia F, Salomão MQ, Bühren J, Roberts CJ, et al. Integration of Scheimpflug-Based Corneal Tomography and Biomechanical Assessments for Enhancing Ectasia Detection. Journal Refract Surg. 2017;33(7): 434–443.
12. Kataria P, Padmanabhan P, Gopalakrishnan A, Padmanaban V, Mahadik S, Ambrósio R Jr. Accuracy of Scheimpflug-derived corneal biomechanical and tomographic indices for detecting subclinical and mild keratectasia in a South Asian population. J cataract refract surg.2019;45(3):328–336.
13. Zhang M, Zhang F, Li Y, Song Y, Wang Z. Early Diagnosis of Keratoconus in Chinese Myopic Eyes by Combining Corvis ST with Pentacam. Curr Eye Res. 2020;45(2): 118–123.
14. Song P, Yang K, Li P, Liu Y, Liang D, Ren S, et al. Assessment of Corneal Pachymetry Distribution and Morphologic Changes in Subclinical Keratoconus with Normal Biomechanics. Biomed Res Int. 2019;2019: 1748579.
15. Rabinowitz Y. Computer-assisted corneal topography in keratoconus. Refract Corneal Surg. 1989;5(6): 400–408.
16. Li X, Rabinowitz YS, Rasheed K, Yang H. Longitudinal study of the normal eyes in unilateral keratoconus patients. Ophthalmology. 2004;111(3): 440–446.
17. Vinciguerra R, Ambrósio R Jr, Roberts CJ, Azzolini C, Vinciguerra P. Biomechanical Characterization of Subclinical Keratoconus Without Topographic or Tomographic Abnormalities. J Refract Surg. 2017;33(6): 399–407.

18. Ucakhan OO, Cetinkor V, Ozkan M, Kanpolat A. Evaluation of Scheimpflug imaging parameters in subclinical keratoconus, keratoconus, and normal eyes. J Cataract Refract Surg. 2011;37: 1116–24.
19. Konstantopoulos A, Hossain P, Anderson DF. Recent advances in ophthalmic anterior segment imaging: a new era for ophthalmic diagnosis. Br J Ophthalmol. 2007;91: 551–7.
20. Ambrósio R Jr, Lopes B, Faria-Correia F, Vinciguerra R, Vinciguerra P, Elsheikh A, et al. Ectasia Detection by the Assessment of Corneal Biomechanics. Cornea. 2016;35(7): e18-20.
21. Wahba SS, Roshdy MM, Elkitkat RS, Naguib KM. Rotating Scheimpflug Imaging Indices in Different Grades of Keratoconus. J Ophthalmol. 2016;2016: 6392472.
22. Belin MW, Villavicencio OF, Ambrosio RR, Jr. Tomographic parameters for the detection of keratoconus: suggestions for screening and treatment parameters. Eye Contact Lens. 2014;40(6): 326–30.
23. Sedaghat MR, Momeni-Moghaddam H, Ambrósio R Jr, Heidari HR, Maddah N, Danesh Z, et al. Diagnostic Ability of Corneal Shape and Biomechanical Parameters for Detecting Frank Keratoconus. Cornea. 2018;37(8): 1025–1034.
24. Wang YM, Chan TCY, Yu M, Jhanji V. Comparison of Corneal Dynamic and Tomographic Analysis in Normal, Forme Fruste Keratoconic, and Keratoconic Eyes. J Refract Surg. 2017;33(9):632–638.
25. Scarcelli G, Besner S, Pineda R, Yun SH. Biomechanical characterization of keratoconus corneas ex vivo with Brillouin microscopy. Invest Ophthalmol Vis Sci. 2014;55:4490–4495.
26. Salomao MQ, Correia FF, Ramos I, Luz A, Ambrosio R Jr. Corneal deformation response with dynamic ultra-high-speed Scheimpflug imaging for detecting ectatic corneas. Int Keratoconus Ectatic Corneal Dis. 2016;5:1–5.
27. Ye C, Yu M, Lai G, Jhanji V. Variability of Corneal Deformation Response in Normal and Keratoconic Eyes. Optom Vis Sci. 2015;92(7):149–53.
28. Vinciguerra R, Ambrósio R Jr, Elsheikh A, Roberts CJ, Lopes B, Morenghi E, et al. Detection of Keratoconus With a New Biomechanical Index. J Refract Surg. 2016;32(12): 803–810.
29. Zadnik K, Steger-May K, Fink BA, Joslin CE, Nichols JJ, Rosenstiel CE, et al. Between-Eye Asymmetry in Keratoconus. Cornea. 2002;21(7): 671–679.
30. Chan TCY, Wang YM, Yu M, Jhanji V. Comparison of Corneal Tomography and a New Combined Tomographic Biomechanical Index in Subclinical Keratoconus. J Refract Surg. 2018; 34(9):616–621.
31. Gomes JA, Tan D, Rapuano CJ, Belin MW, Ambrósio R Jr, Guell JL, et al. Global consensus on keratoconus and ectatic diseases. Cornea. 2015;34(4): 359–69.
32. Imbornoni LM, Padmanabhan P, Belin MW, Deepa M. Long-Term Tomographic Evaluation of Unilateral Keratoconus. Cornea. 2017;36(11): 1316–1324.

Figures

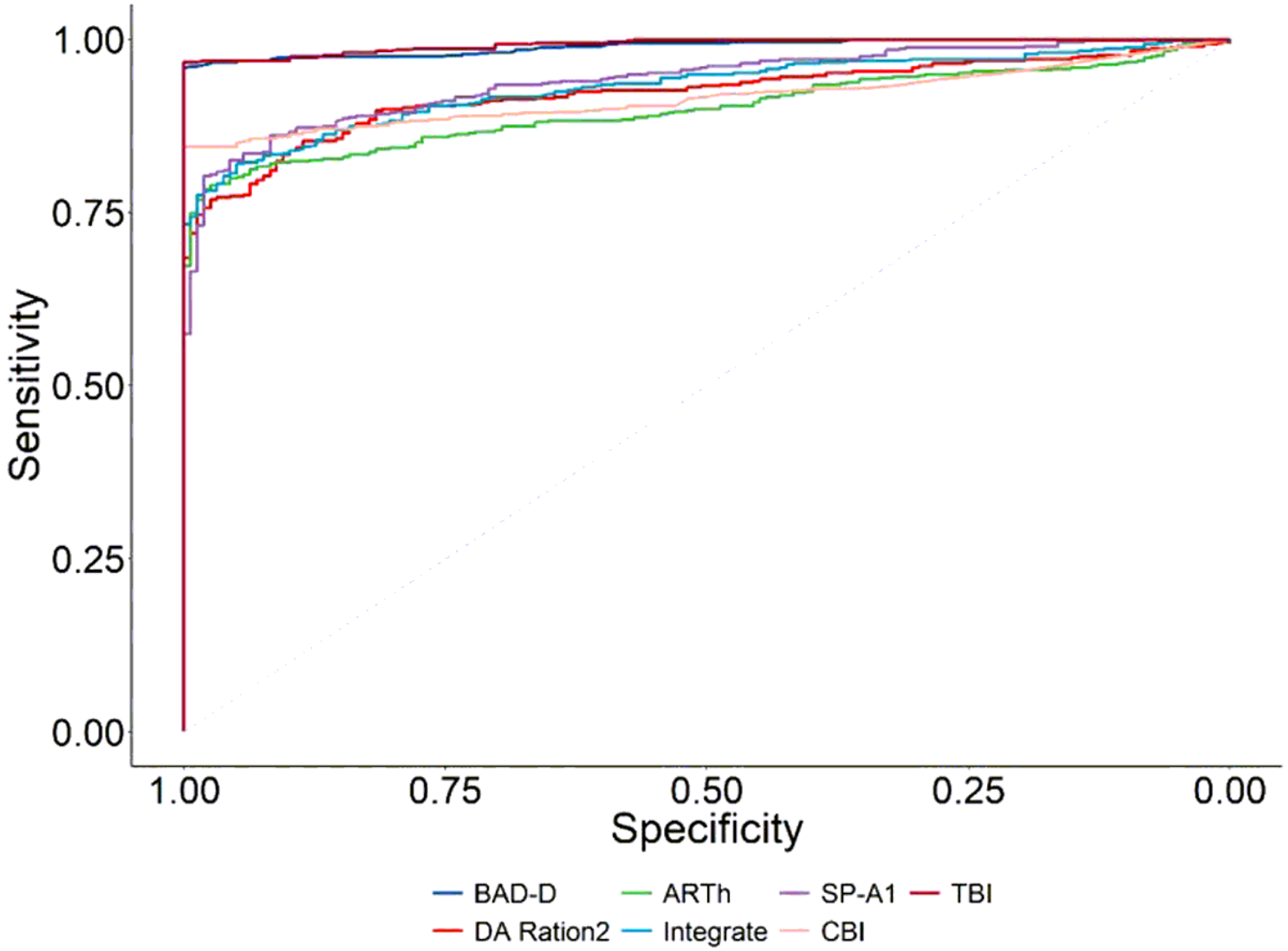

Figure 1

Receiver operator characteristic curve for distinguishing keratoconus from normal corneas.

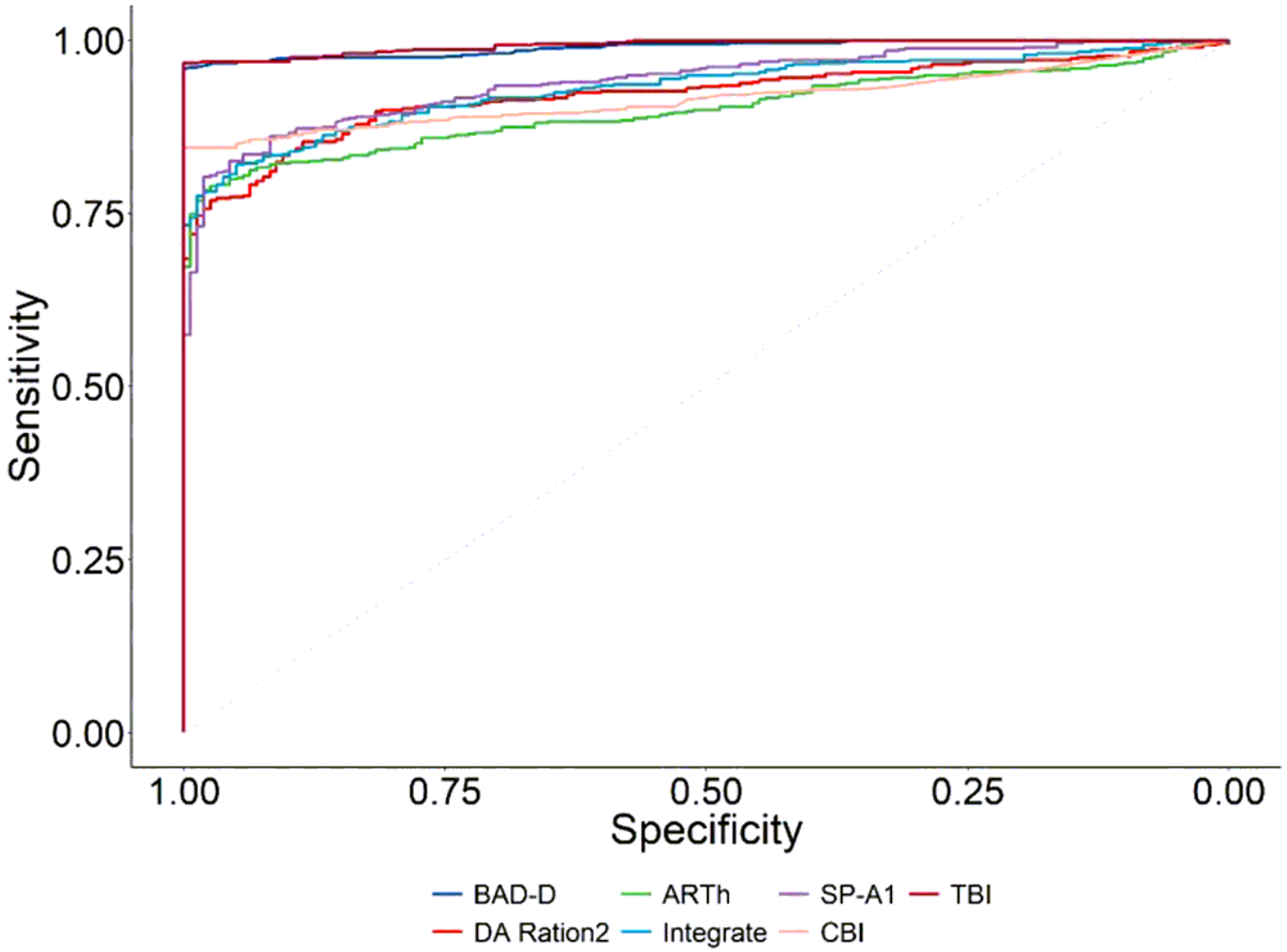

Figure 1

Receiver operator characteristic curve for distinguishing keratoconus from normal corneas.

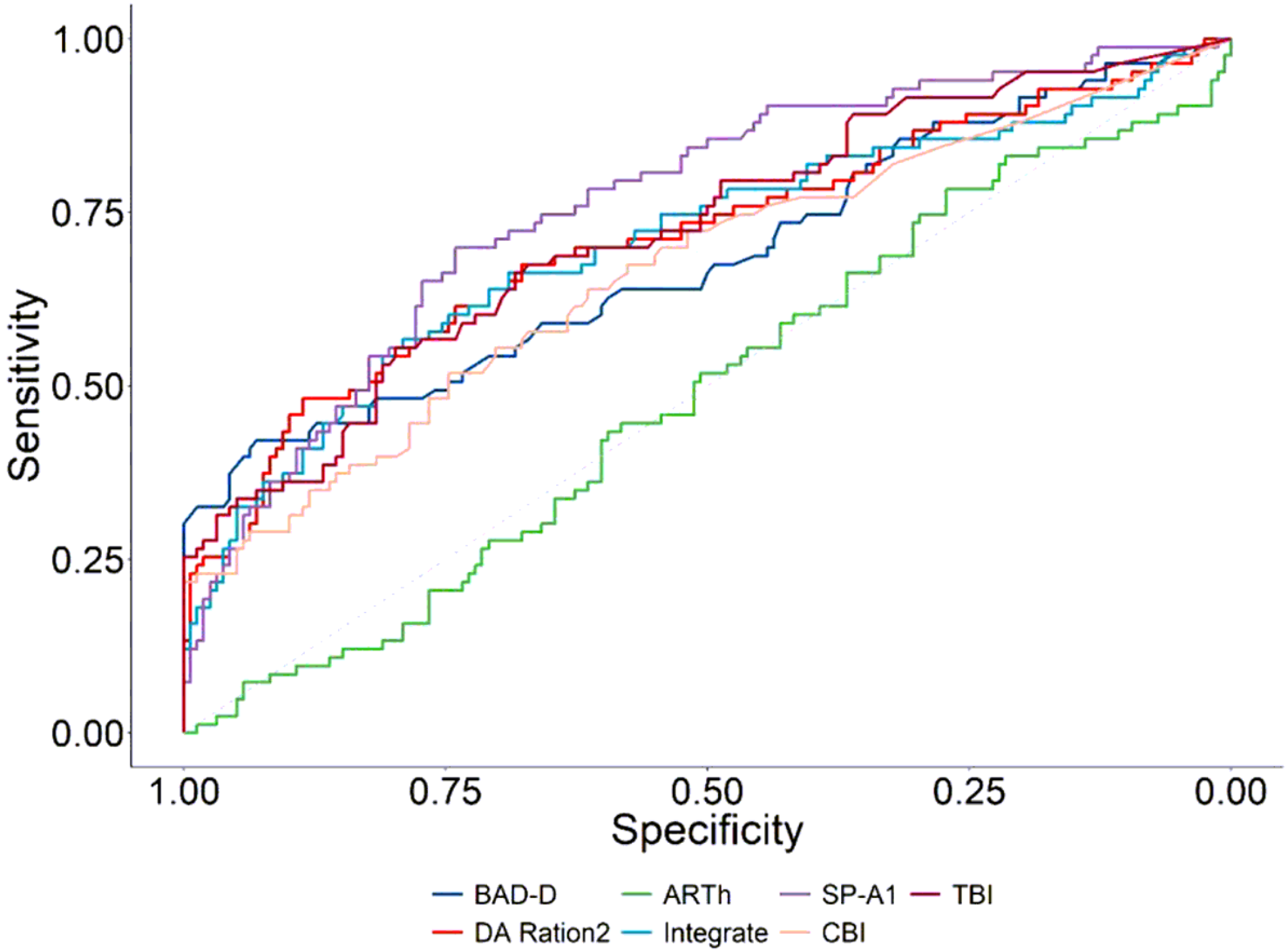

Figure 2

Receiver operator characteristic curve for distinguishing forme fruste keratoconus from normal corneas.

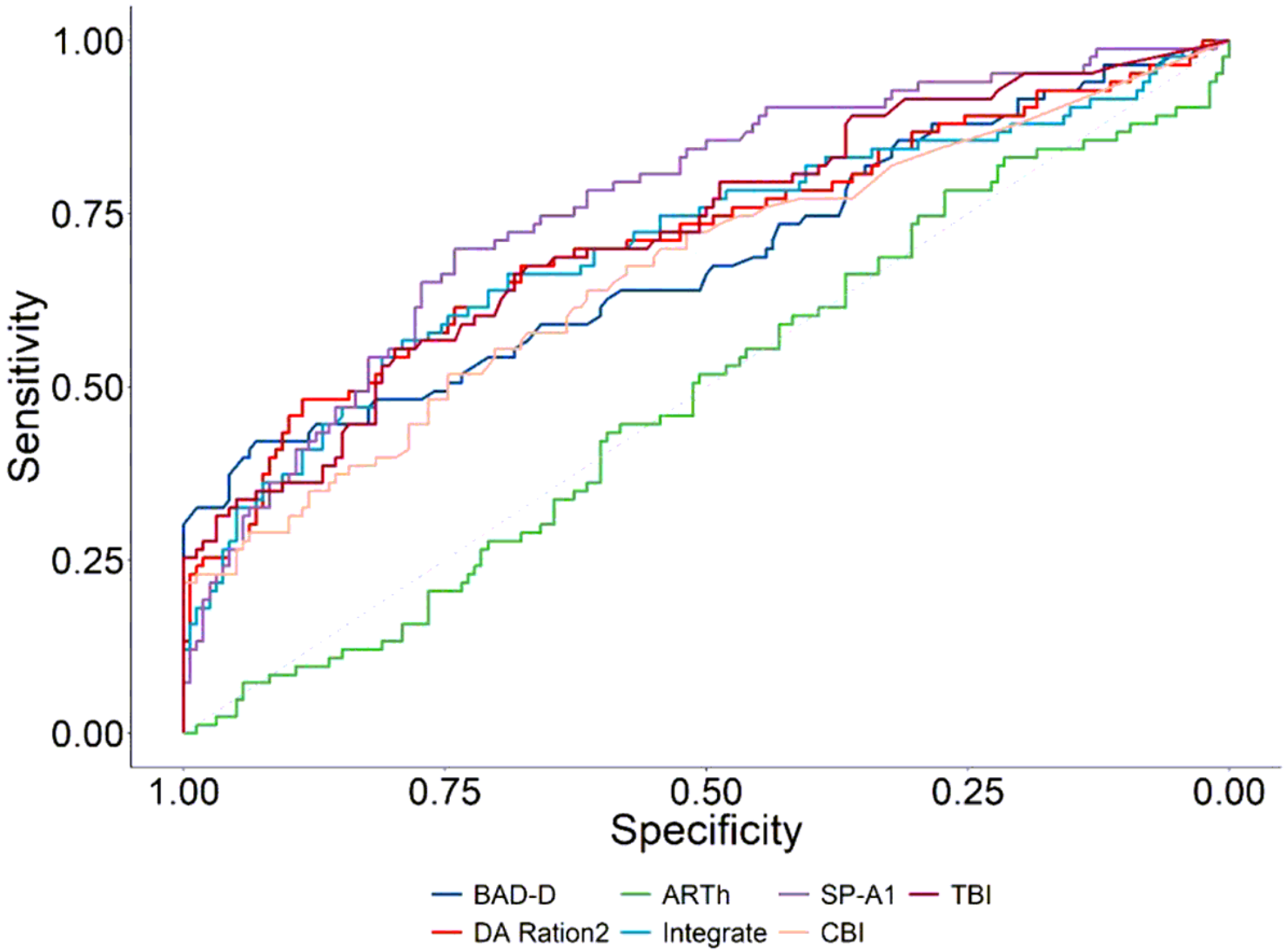

Figure 2

Receiver operator characteristic curve for distinguishing forme fruste keratoconus from normal corneas.